Reliability-Based Fatigue Monitoring of Fracture Critical Structures

Eric M. Hernandez

7th European Workshop on Structural Health Monitoring
July 8-11, 2014. La Cité, Nantes, France

RELIABILITY-BASED FATIGUE MONITORING OF FRACTURE CRITICAL STRUCTURES

Eric M. Hernandez[1]

[1] *College of Eng. and Math. Sciences, University of Vermont. Burlington, Vermont, USA*

eric.hernandez@uvm.edu

ABSTRACT

This paper presents a finite element model-based state observer, which allows for accurate real time monitoring of stress, strain and their resultants at any location within an instrumented structure. The input to the proposed observer is: a finite element model of the structure, the spectral density matrix of the random field representing the loading environment and noise contaminated measurements of structural response. The resulting observer operates as a modified version of the original FEM of the structure driven by the measured response of the system. Using the rain flow cycle counting algorithm along with existing fatigue damage models, observer estimates are used to compute the number and amplitude of stress and strain cycles and the cumulative fatigue damage at critical points of the structure. These estimates can be used to obtain reliability estimates of the current state of the structure and prognosis under projected conditions.

KEYWORDS : *Fatigue, Monitoring, Damage, State estimation, Kalman filter*

1 INTRODUCTION

Fatigue is a phenomenon that takes place in components and structures subjected to time-varying external loadings and that manifests itself in the deterioration of the material's ability to carry the intended loading [1]. Fatigue damage is characterized as a non-decreasing function of the number of stress cycles across the range of amplitudes. Fatigue failure can occur as a byproduct of a low number of cycles (< 1000 load cycles) at a high stress range or high number of cycles at low level of stress. In high-cycle fatigue, one can typically distinguish three sequential damage phases: (i) nucleation, (ii) micro-crack and (iii) macro-crack growth. Some damage functions try to differentiate between phases and others simply aim at characterizing the number of cycles until failure. The most commonly used high-cycle fatigue damage function is the Miner-Palmgren rule [2, 3], which postulates that damage (D) accumulates as

$$D = \sum_i \frac{n_i}{N_i} \tag{1}$$

where N is the number of cycles to failure and n is the number of cycles experienced by the component. The sub-index "i" stands for the stress cycle amplitude S_i. Failure is assumed to occur if $D>1$. Many other fatigue models have been proposed however due to its simplicity and relative effectiveness with respect to other models, the Miner-Palmgren rule remains popular. The number of cycles to failure (N_i) for a given stress range S_i are commonly represented as a power law (Basquin model) of the form

$$N = kS^{-b} \tag{2}$$

where k and b are constants determined experimentally and S is the stress range. It is well documented that there is significant uncertainty on the values of N, b and k (Sobczyk & Spencer, 1992), thus fatigue is a fundamentally a random phenomenon.

In fatigue monitoring applications, two problems typically arise: (i) determining the critical locations where significant fatigue damage will take place and (ii) one cannot monitor all locations of interest. The problem of identifying potential locations of origination of fatigue cracks is extremely challenging and stochastic in nature since it depends on initial fabrication defects, and other imponderable variables. However, the usage monitoring problem is more tractable and various authors have proposed methods to use of sparse measured vibration response as a means to monitor stresses and fatigue damage throughout the complete structures without deterministic knowledge of the excitations [4, 5]. The basic premise is that by using measured structural response one can improve upon purely stochastic estimates that do not use measurement feedback. The proposed approach relies on state estimation [6].

Once the time history of the states (displacement and velocity at all degrees of freedom) is estimated, the stress resultants and any damage function of them can be readily obtained as functions of the estimated state. Therefore the problem of stress reconstruction can be cast as tracking problem where the estimated damage condition (diagnosis) can be performed with its uncertainty and the reliability of the structure to fatigue can be estimated. The current state of damage can also be projected into the future together with its uncertainty to perform prognosis.

For linear dynamical systems with unmeasured excitations which are realizations of white Gaussian noise and the measurements contaminated with realizations of white Gaussian noise; the Kalman filter [7] is the optimal state estimator in the sense that it minimizes the Euclidian norm of the estimation error. However, in the case of structural engineering applications, the loading, in violation of the standard KF assumptions, can exhibits significant spatial and temporal correlation and it is not evident that the KF will provide accurate estimation under these conditions. In addition, for second-order mechanical systems some issues arise regarding the internal consistency of the state vector estimation when a KF is used. These issues have been discussed in detail in [8, 9].

This paper proposes a finite element model based estimator (MBE) that can be realized as modifications of a finite element model of the system subject to corrective forces that drive the modified system towards the true state [8]. The proposed estimator allows for explicit consideration of unmeasured stationary loads modelled as realizations of a random field with specified spectral density and spatial correlation. In this paper we look at the specific case of wind loading.

The paper begins with an introductory section describing the assumed system model followed by a section describing the stochastic load model. The next section describes the proposed FEM based estimator. A section presenting the stochastic simulation results and a comprehensive comparison between the KF estimates, stochastic estimates and the proposed model based estimator concludes the paper.

2 SYSTEM MODEL

Throughout the paper, we shall restrict our attention to symmetric, finite and *n*-dimensional linear structural systems obeying Newton's equation of motion with velocity proportional damping described by the following matrix ordinary differential equation

$$\mathbf{M}\ddot{q}(t) + \mathbf{C}_{\mathbf{D}}\dot{q}(t) + \mathbf{K}q(t) = \mathbf{b}_2 f(t) \tag{3}$$

where $q(t) \in R^{n\,x\,1}$ is the displacement vector at time t, $\mathbf{M} = \mathbf{M}^T > 0$ is the mass matrix, $\mathbf{C}_D = \mathbf{C}_D^T \geq 0$ is the damping matrix, and $\mathbf{K} = \mathbf{K}^T \geq 0$ is the stiffness matrix. The forcing function vector is $f(t) \in R^{n\,x\,1}$ and $\mathbf{b}_2 \in R^{n\,x\,n}$ is the force distribution matrix, which indicates the degrees of freedom on which the forcing function is applied. Measurements of the system's response are given by

$$y(t) = \mathbf{C}x(t) + \mathbf{D}f(t) + v(t) \tag{4}$$

where $\mathbf{C} \in R^{m\,x\,2n}$ is the measurement matrix and $v(t) \in R^{m\,x\,1}$ is the measurement noise. For the purposes of this paper, the simulated system is a cantilevered slender vertical structure with a height of 100m and a tapered hollow circular cross section which varies from 5.0m at the base to 2.5m. at the top with wall thickness of 0.305m. The finite element model of the structure is discretized every 5.00m with a total of 20 elements across the height. The structure is modeled as steel with elastic modulus of 210,000 MPa and 1% classical damping in every mode. The resulting fundamental frequency of the structure is 0.30 Hz. In addition to the wind induced forces throughout the height, the top the structure has a wind-induced concentrated force (similar to what would occur in a wind turbine or sign structure). Measurements of structural response to be used as feedback consists of velocities at z=50m and z=100m.

2.1 Numerical simulation of stochastic loads

For the vertical structure investigated in this paper, the stochastic loads consist of lateral wind pressure. The wind velocity field is modeled as one-directional; for every nodal point in the finite element model a load time history (fluctuating component of wind) is simulated from a synthetically generated turbulence field in accordance with the quasi-steady assumption, the Kaimal spectrum and the corresponding PSD matrix of turbulence computed at various discrete points [10]. The results presented here are related to the time varying portion of the wind load (turbulence), and thus the purely static effects are not shown. For the wind simulations a density of air of 1.20kg/m^3 was used and a constant drag coefficient of 1.20, corresponding to circular sections (Reynolds number effects were neglected). The wind parameters that define the Kaimal spectrum are selected as z_o=0.1, U=30 m/s and C_z=10.

For purposes of illustration, Fig.1 depicts one specific realization of the turbulence wind velocity at four representative heights (25, 50, 75 and 100 m) at U=30 m/s. To realize the Kaimal spectrum as a digital time signal the algorithm proposed by [11] was employed. The algorithm is based on a spectral decomposition of the power spectral density matrix of the fluctuating wind turbulence at discrete points ($u_j(t)$) and superposition of a finite series of harmonic waves with amplitude evaluated from actual turbulence PSD and a uniform random phase. For the simulations presented in Fig. 1, the number of waves selected for the spectral decomposition was 10,000; the upper cut-off frequency was 50 Hz and the time step 0.01 s.

3 MODEL BASED OBSERVER

The proposed FEM based estimator presented in this paper was originally derived by [8] and in the case of velocity feedback measurements it is written in second order form as,

$$\mathbf{M}\,\ddot{\hat{q}}(t) + \left(\mathbf{C}_D + \mathbf{c}_2^T\mathbf{E}\mathbf{c}_2\right)\dot{\hat{q}}(t) + \mathbf{K}\,\hat{q}(t) = \mathbf{c}_2^T\mathbf{E}\,y(t) \tag{5}$$

As can be seen from eq.5, the proposed estimator becomes a modified version of the system with added dampers and excited by forces which are linear combinations of the output measurements and proportional to the added dampers. The basic component of the proposed estimator is the matrix **E** which must be selected to minimize the trace of the state error covariance.

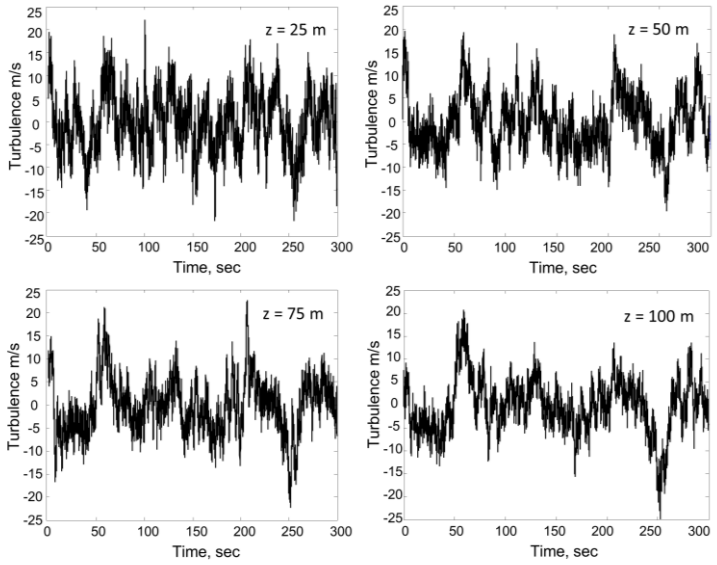

Figure 1. Realization of synthetically-generated time history of turbulent wind velocity field (along-wind component) at various heights (z=5, 10, 15, 20 m) along the structure; U = 30 m/s.

Defining the state error as $e = q - \hat{q}$, the expression for the state error is given by

$$\mathbf{M}\,\ddot{e}(t) + \left(\mathbf{C}_D + \mathbf{c}_2^T\mathbf{E}\mathbf{c}_2\right)\dot{e}(t) + \mathbf{K}\,e(t) = \mathbf{b}_2 f(t) - \mathbf{c}_2^T\mathbf{E}\,v(t) \tag{6}$$

where **E** is still free to be selected. It is evident that as the matrix **E** increases the effective damping of the estimator increases and consequently reduces the estimation error. However, it also increases the term driving the estimation error on the right hand side of eq.6, which is proportional to the measurement noise. Therefore, an optimal balance should be reached in order to make the optimal choice for **E.** A detailed derivation of the optimization function required to obtain **E** is given in [8]

4 IMPLEMENTATION OF MODEL BASED OBSERVER

For a general multivariable case an analytical closed-form solution for the optimal matrix **E** has not been found; therefore, numerical optimization is required. However such minimization is not numerically expensive because, although $(m^2+m)/2$ independent values are theoretically required to uniquely define **E**; using only m (the diagonal of **E**) can yield acceptable results. Physically, this

means that the estimator model would only require added grounded and corrective forces collocated with the measurements, and no dashpots interconnecting the output locations.

Finally, it is important to note that it is theoretically possible to formulate the estimator based on displacement or acceleration measurements. Both cases are shown explicitly in [8]. In this paper, we focus on velocity feedback mainly because the resulting estimator possesses the same fundamental undamped frequencies and mode shapes as the system.

4.1 Computing the Model-Based Observer

To compute the proposed model-based state observer the feedback matrix **E** must be estimated based upon minimization of eq. 6. As has already been argued in a previous section and based on a physical interpretation of the proposed estimator; the matrix **E** can be taken as a diagonal 2 x 2 matrix. The physical interpretation of this choice in the context of the structure considered in this study is presented in Fig. 3.

The optimization was performed within the MATLAB® environment using the `fminsearch` function. This function uses the Nelder-Mead simplex algorithm as described in [12]. The parameters used in the optimization function were `xTol=`10^{3} and `FunTol=`10^{-9}. The optimization was started at $\beta_1 = 0$ and $\beta_2 = 0$. In addition, we added a small penalty term to prevent unnecessary high values of the **E** matrix without significant increase in function accuracy. The modified optimization function used was

$$J_2 = J_1 + 10^{-17} tr(\mathbf{E}) \tag{7}$$

The minimum found by the optimization algorithm was

$$\mathbf{E} = \begin{bmatrix} \beta_1 & 0 \\ 0 & \beta_2 \end{bmatrix} = 10^{7} \begin{bmatrix} 1.0697 & 0 \\ 0 & 0.6641 \end{bmatrix} \tag{8}$$

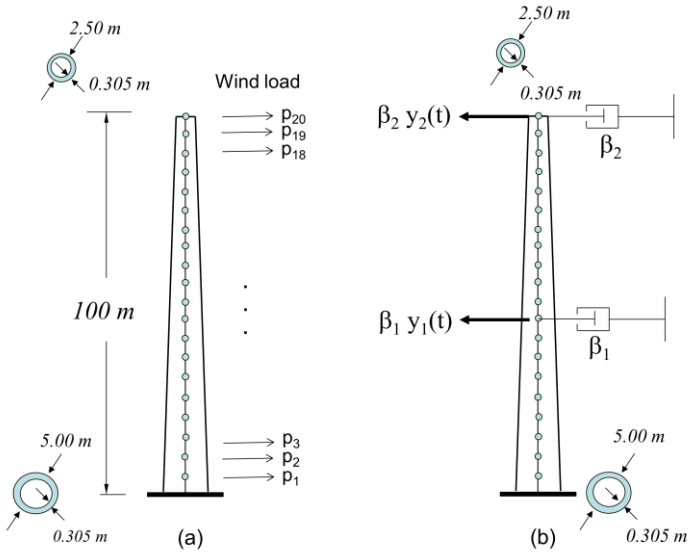

Fig.3. (a) Dimensions, discretization and loads (b) FEM-estimator

To assess convexity we selected various starting points in the optimization algorithm, in addition to the original $\beta_1 = 0$ and $\beta_2 = 0$. We found that $\beta_1 = 10^4$ and $\beta_2 = 10^4$, $\beta_1 = 10^4$ and $\beta_2 = 0.2 \times 10^4$, $\beta_1 = 0.2 \times 10^4$ and $\beta_2 = 10^4$ all converge to the same solution. Therefore, although we cannot assess convexity analytically, we can reasonably say under a range of choices of initial conditions the function converges to a unique minimum.

4.2 Estimator Performance - Statistical Analysis of Results

In order to assess the relative accuracy of both estimators (KF and the proposed estimator) 500 random simulations of 300 seconds duration each are performed. In these simulations, the tracking capability and estimation of the number of threshold crossings at various levels of demands are compared. For each simulation the target wind spectrum remains constant, however due to the method of simulation, each harmonic component of along-wind turbulence has a random phase and, thus, for each simulation the time history of the loading is different. Also, load modeling error is implicitly included in the simulations, since the simulated wind does not exactly match the target wind spectrum due to truncation of the synthetically-generated turbulence records to a finite series of harmonics, the inherent discretization of the spectrum along the frequency axis and the finite-length records in the time domain. This makes the results more realistic and useful for verification of the proposed algorithm in realistic applications. The results to follow are presented for the bending moment at the base of the cantilever (critical section).

Fig.4. illustrates a comparison between the time histories of the true system response, the proposed Model Based Estimator (MBE) and the Kalman Filter (KF) for one of the 500 simulations. The estimation error for both methods is also shown in the bottom. The estimation error of the MBE is generally smaller than the estimate provided by the KF. Fig.5 illustrates the accuracy of the proposed state observer to estimate the mean number of threshold crossings for various level of bending moment at the base.

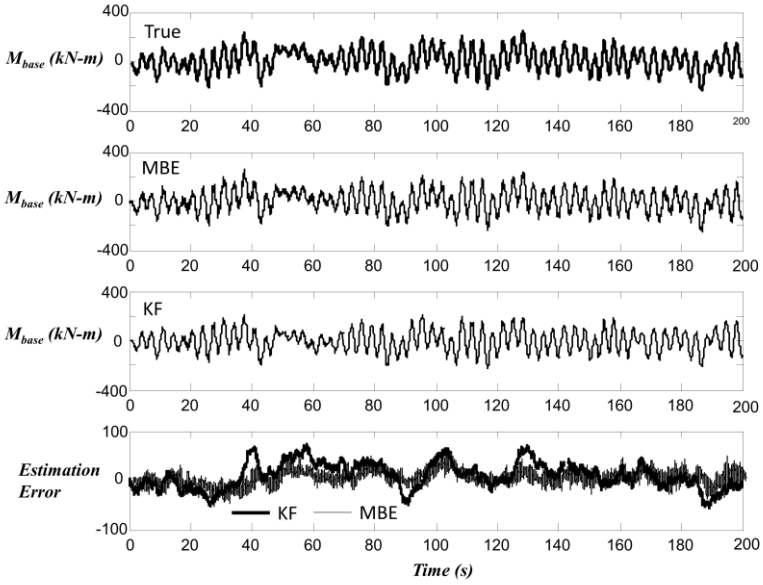

Fig.4. Comparison of bending moment estimates at the base of the structure.

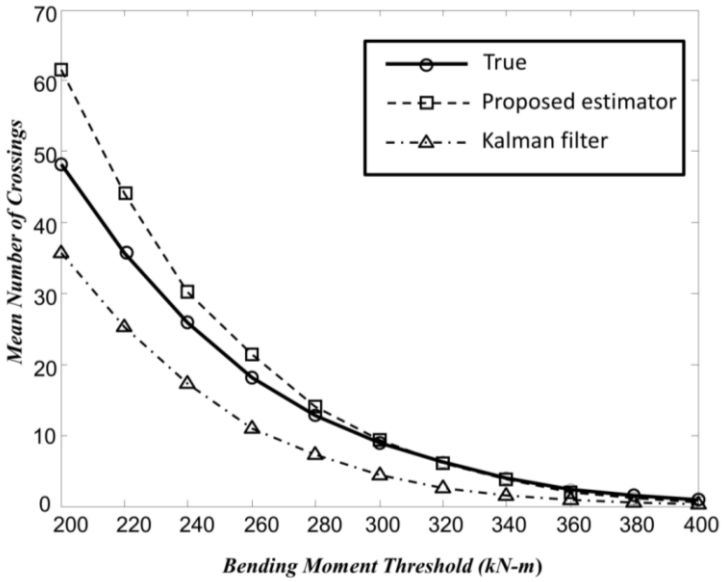

Figure5. Mean number of threshold crossings for the simulated system ("True"), the proposed model-based estimator and the KF.

4.3 Fatigue Damage Analysis

To perform a damage assessment we simulated 10 minutes of data, and used the proposed FEM-based observer to compute the stress time history at the base of the cantilever. With the estimated time history of stress, we can compute the number of stress cycles using the rainflow counting algorithm (see Fig.6) and use eqs.1 and 2 to obtain an estimate of the fatigue damage induced during the simulated time. The results are compared with the true damage (computed using the assumed unknown stress time history), the KF estimate and the stochastic estimate given by [13] which does not use measurement feedback.

Table 1. Comparison of Fatigue Damage Results for T=600s.

	ΣN	D ($x10^{-11}$)
System Response	920	8.38
MBO	818	8.38
KF	817	8.18
Stoch. Estimate	1157	12.03

5 CONCLUSIONS

The paper treats the problem of tracking cumulative fatigue damage in fracture critical structures subjected to unmeasured time-varying excitations, assumed to be realizations of random fields with known power spectral density matrices. The approach presented here relies on the estimation of the time history of the stress fields throughout the structure and using those as input to fatigue damage functions. It was found by means of simulations that the proposed model-based estimator outperforms a standard Kalman filter in both tracking and estimating the number of crossings at all levels considered. It was also found that both the KF and the proposed Model-based observer outperform purely stochastic estimates significantly, even though only two measurements are used as feedback. The estimated damage metric can be used as an assessment tool to diagnose the current

state of damage of the structure and to perform prognosis in order to determine the probability of failure at a future time.

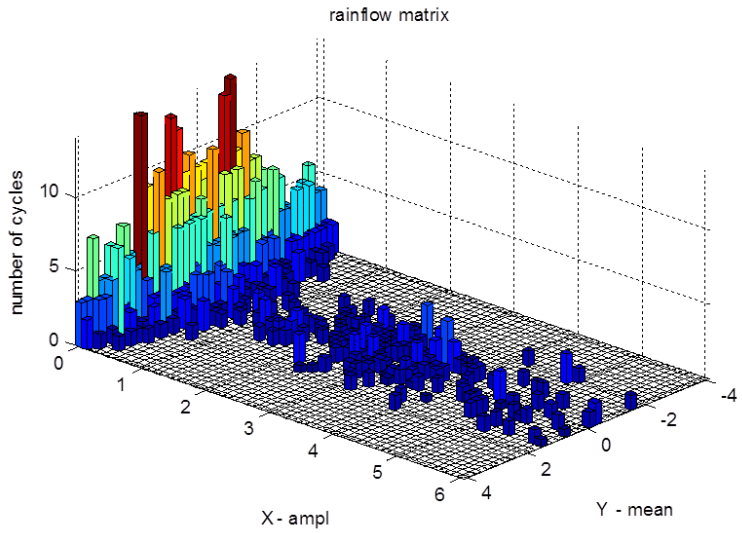

Fig.6. Estimated rainflow matrix for the number of stress cycles as a function of mean and amplitude of the cycle (T=600 s).

6 REFERENCES

[1] Sobczyk, K. and Spencer, B.F. 1992. Random Fatigue: From data to theory. Academic Press Inc. Boston, MA.

[2] Miner, M.A. 1959. Estimating fatigue life with particular emphasis on cumulative damage. In Metal Fatigue, McGraw-Hill Inc. New York, NY.

[3] Palmgren, A. 1924. Die Lebensdauer von Kugellagern, Zeitschrift des Vereines, Deutsches Ingenieure, Duesseldorf, Germany, 68(14)

[4] Hernandez, E.M., Bernal, D. and Caracoglia, L. 2012. On-line Monitoring of Wind Induced Stresses and Fatigue Damage in Structures. *Journal of Structural Control and Health Monitoring* DOI: 10.1002/stc.1536

[5] Papadimitriou, C., Fritzen, C-P., Kraemer, P., Ntotsios E. 2010. Fatigue predictions in entire body of metallic structures from a limited number of vibration sensors using Kalman filtering. *Journal of Structural Control and Health Monitoring* 18(5): 554-573.

[6] Simon, D. 2006. Optimal State Estimation. John Wiley and Sons, New York, NY.

[7] Kalman R.E. 1960. A new approach to linear filtering and prediction problems. *Trans. ASME, Jour. of Basic Engr.* 82(1): 35-45.

[8] Hernandez, E.M. 2013. Optimal Model Based State Estimation in Mechanical and Structural Systems. *Journal of Structural Control and Health Monitoring* 20:532-543

[9] Balas, M.J. 1999. Do all linear flexible structures have convergent second-order observers? AIAA Journal of Guidance Control and Dynamics 22 (6):905–908

[10] Simiu, E. and Scalan, R. 1996. Wind Effects on Structures. John Wiley and Sons Inc. New York, NY.

[11] Di Paola, M. 1998. Digital simulation of wind field velocity. *Journal of Wind Engineering and Industrial Aerodynamics*, 74-76: 91-109

[12] Lagarias, J.C., J. A. Reeds, M. H. Wright, and P. E. Wright, 1998. Convergence Properties of the Nelder-Mead Simplex Method in Low Dimensions. SIAM Journal of Optimization, Vol. 9 Number 1, pp. 112-147

[13] Holmes, J. D. 2002. Fatigue life under along-wind loading - closed-form solutions. *Engineering Structures*, 24(1): 109-114